Chapter 3 Experimental procedures and results

3.1 Lateral grain growth induced by metal reflection layer

The full fabrication process steps are shown in figure 3.1 (a) .First, we deposited the 50nm SiN_X and 100nm SiO_2 on the glass substrate cleaned previously as the buffer layer which we mentioned before by plasma enhanced chemical vapor deposition (PECVD), and the 50nm and 100nm α-Si film was deposited on the buffer layer by PECVD separately. The α-Si was annealed at $490^{O}C$ for 8 minutes to dehydrogenation. Dehydrogenation is a method to remove the hydrogen in the silicon film during the PECVD process shown in Figure 3.2. If the hydrogen in the α-Si film was not removed before the laser crystallization the covalence bond of Si-H would be destroyed. The hydrogen atoms combines to form hydrogen molecules and the molecules would burst out of the silicon film. It's hydrogen explosion and does a serious damage on the film surface. The 100nm metal Cr was deposited by sputter with the rate of 1Å m/sec and patterned in to an island shape by photolithography. Finally, a XeF laser (wavelength is 351nm) irradiated on the sample with ten shots and the laser intensity is 200 to 400 mJ/cm^2 with each step of 50 mJ/cm^2. The laser instrument is shown in figure 3.1 (b). The convex lens and the reflection mirror are made for UV wavelength and the laser intensity is tuned by the position of the convex lens. The experiment is processed in the atmosphere but not in a vacuum environment and it would induce the film quality decreasing and the surface roughness increasing.

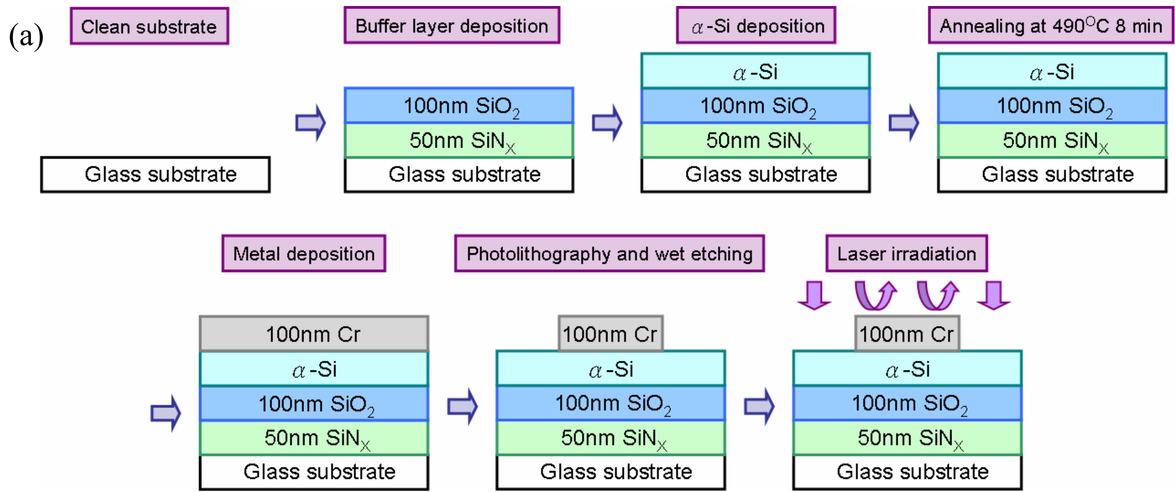

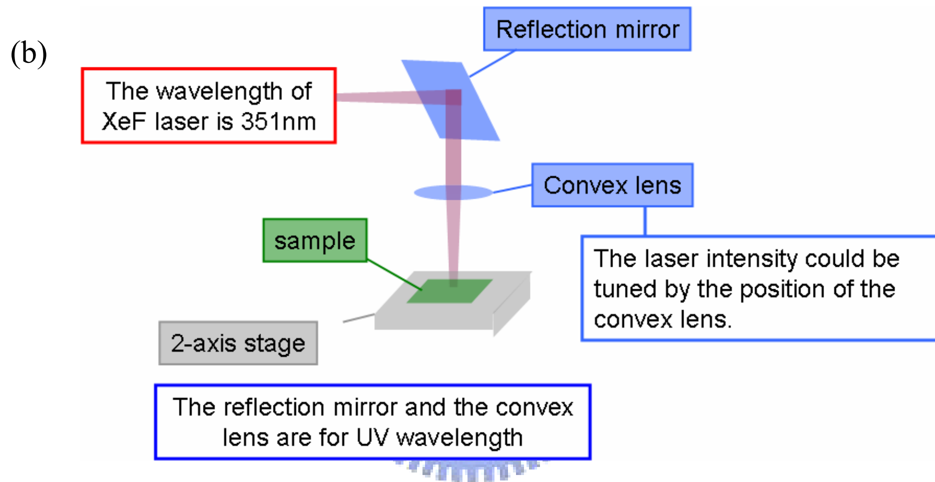

Figure 3.1 (a) Full fabrication process of the metal reflection layer including the sample preparation and laser irradiation. (b) The laser instrument.

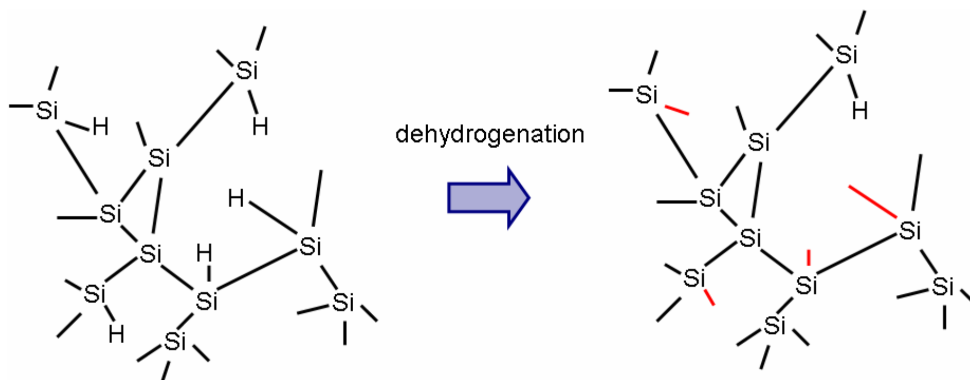

Figure 3.2 The left figure is the silicon film before dehydrogenation, the right is the silicon after dehydrogenation and the red lines represent the bond destroyed in the dehydrogenation.

After irradiation, we observed the metal patterns on the sample and find that the metal was split off at the energy intensity higher than 300mJ/cm^2 (shown in figure 3.3) such that the metal would not be able to block the following laser pulses. The sample was secco-etching which can remove the defects in the silicon for 90 seconds. In figure 3.4, the lateral grain growth phenomena can be observed near the edge of the metal reflection pattern. The average lateral grain size is about 1.3 times the grains near the lateral grain growth region and the grain growth direction is perpendicular to the edge of the reflection pattern. There exists a distance about 1μm between the metal and the grain growth nuclei, because during the laser irradiation process the partial laser energy transferred to the a-Si covered by the metal pattern. In the simulation results (shown in figure 2.4), the temperature of the liquid Si near the reflection metal decreased so rapidly such that the random nucleation occurs in that region but not lateral grain growth. It could be observed in figure 3.4 (a), (b) and (c) that at the higher laser energy regime the larger grain size could be obtained. However, when we increased the laser energy higher than 300mJ/cm^2, the shielded metal layer would split off. Due to the short laser pulse duration time about 25ns, the silicon and Cr film received a large amount of laser energy in a short time such that the ablation of the films would take place in a higher irradiation energy regime. For the 1000Å Si film, the lateral grain growth only occurred in laser intensity about equal to 300mJ/cm^2. When the laser intensity is less than 300mJ/cm^2 the laser energy is not large enough to induce a lateral growth (figure 3.4 (e)). If the laser energy is larger than 300mJ/cm^2 the metal film would be split off. Comparing the different Si film thickness we could find that the average grain size of the 500Å Si film is a little larger than that of 1000Å Si film at the same laser intensity 300mJ (shown in figure3.4(c) and (d)). We used the same laser irradiation intensity on the 500Å and 1000Å Si film but actually the average energy per unit volume absorbed by the 1000Å Si film is less that absorbed by the thinner Si film such that the average grain size of the 1000Å Si film is smaller than that of 500Å Si film even at the lateral grain growth region. The average grain size of the thicker silicon film is 0.4 μm.

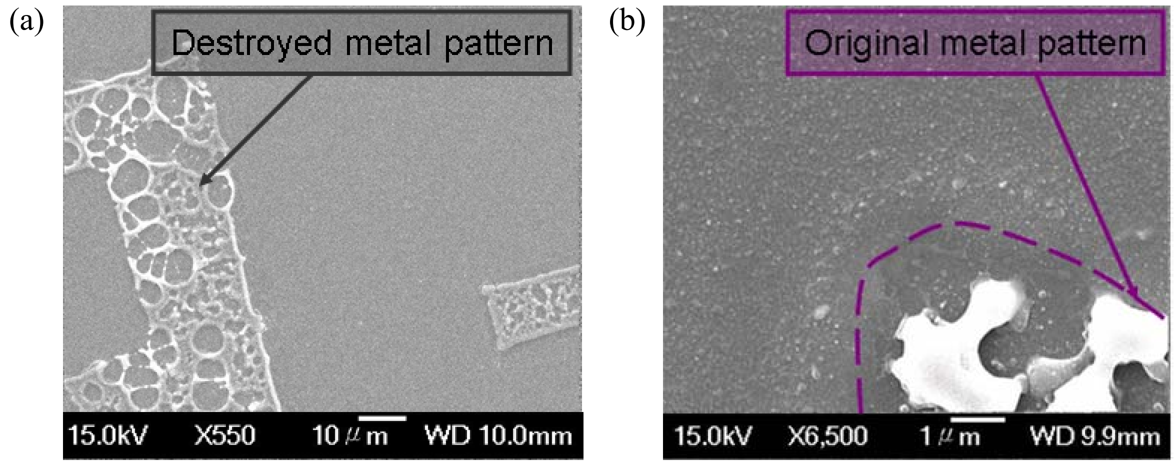

Figure 3.3 The high energy laser is about 400mJ/cm^2 and the original metal pattern was destroyed and split off. (a) The broad view. (b) The fine view.

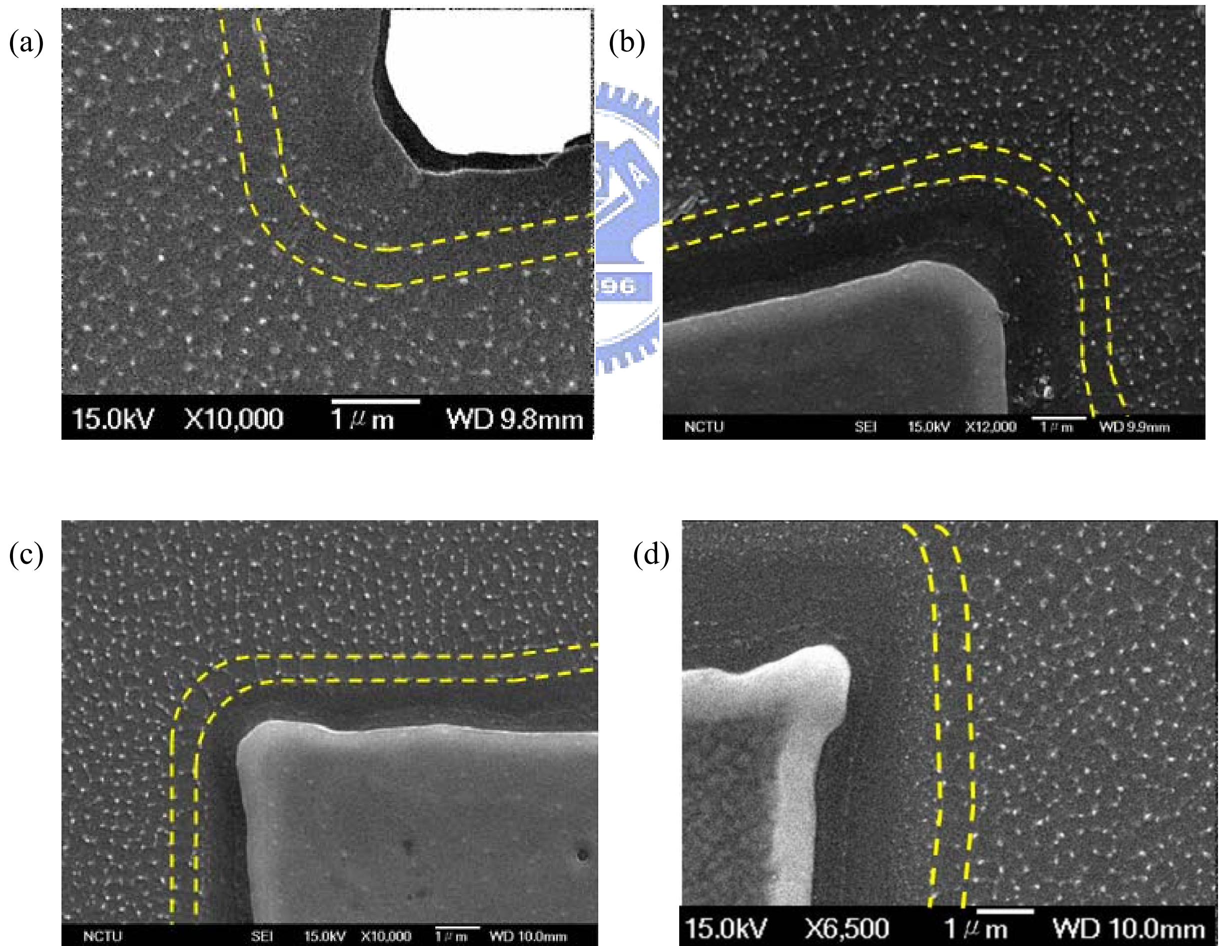

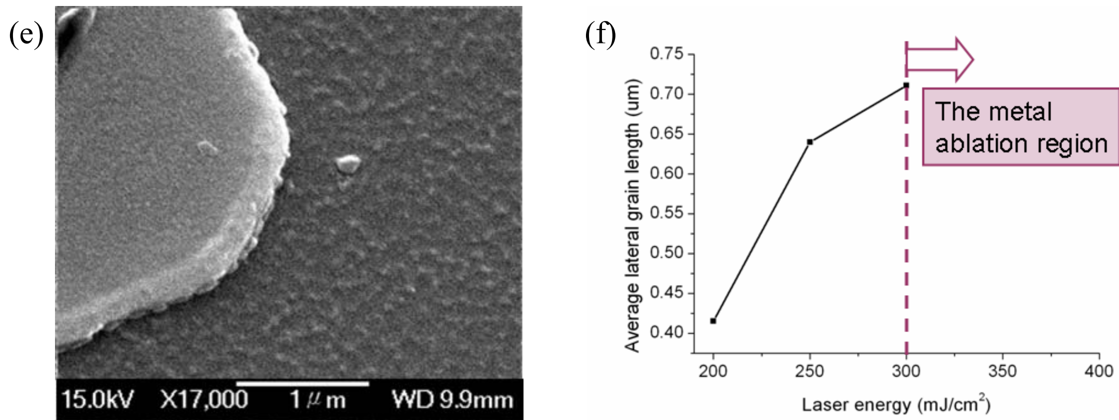

Figure 3.4 SEM image for the lateral growth region after secco-etching and the arrow represents the lateral grain growth length. (a) The laser energy = 200 mJ/cm^2 and the silicon film thickness = 50nm (b) The laser energy = 250 mJ/cm^2 and the silicon film thickness = 50nm (c) the laser energy = 300 mJ/cm^2 and the silicon film thickness = 50nm (d) The laser energy = 300 mJ/cm^2 and the silicon film thickness = 50nm. (e) The laser energy = 250 mJ/cm^2 and the silicon film thickness = 100nm. (f) The curve of lateral grain growth length versus the laser intensity.

The lateral grain growth induced by metal reflection layer is a useful method in controlling the grain size, growth direction. It not only enlarges the grain size than that without reflection pattern but also forms well-arranged grain boundary as we expected. We compared the different laser energy with the same Si film thickness and we find that the lateral grain growth length become larger when we increased the laser intensity as shown in figure 3.4 (f). We also discussed the effects of the Si film thickness with the same irradiation energy. Theoretically the thicker film should induce the larger grain size, but the limit of the laser intensity confine the grain growth length. By changing a new metal material to be the blocking layer the confinement of the laser intensity would be solved and the larger grain growth could be expected.

3.2 Nucleation positions controlled by "nano-holes"

The sample preparation process is shown in figure 3.5. The 1μm buffer layer SiO_2 was deposited on the Si wafer by furnace and we patterned the nano-holes by the e-beam lithography and etching the SiO_2 and the photo-resistance by RIE. The e-beam lithography is the method which could pattern a finer dimension than a normal photolithography. At first, the photo-resistance PMMA was spin-coated on the SiO_2 and then we use the electron beam to exposure the selective region which would be removed later. The 1000Å α-Si was deposited by PECVD. Then the Si film was dehydrogenation by furnace at $490^{O}C$ in 8 minutes and the laser irradiates on the patterned region.

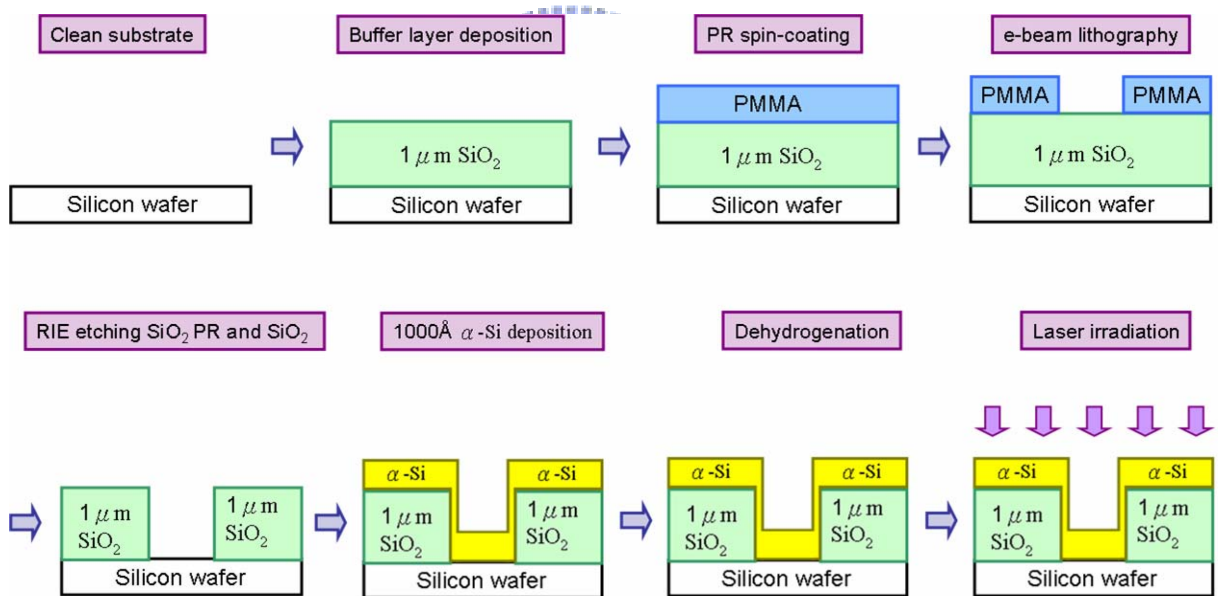

Figure 3.5 Full fabrication process of the nano-hole structure including the sample preparation and laser crystallization.

During the α-Si deposition process, there is a thin silicon film deposition on the sidewall in the nano-holes. When he laser irradiated on the patterned region the thick α-Si film formed on the edge of the nano-holes. We chose the laser energy about $500mJ/cm^2$ that couldn't totally melting the thick Si film but melting the thin Si-film such that nuclei existed in the

edge of the circles. The grain grew from the nuclei to the completely melting region and collided with the other grain growing from the neighbor holes. The grain boundary could be well controlled in the edge of the holes and the middle of the nano-holes. In our designs shown in figure 3.6, the diameter of the holes (D) is 200nm and the distance between the holes (L) is 1μm and 2μm. The average grain size could be controlled as 0.4μm when L is equal to 1μm. In figure 3.7, the grain size is indicated by the circles. When the laser energy increases about 100mJ/cm^2 (comparing (a) and (b)) the grain size still well controlled in the size about 0.4μm. It shows a high-independence of laser energy property and it's useful to broaden the process window. As long as our laser intensity is not large enough to complete melting the thick silicon layer the ability of grain growth length controlling is better than the metal reflection layer. The laser energy is still limited if the laser energy is high enough to induce the ablation of the Si film. This phenomenon could be observed in the figure 3.7 (c). The Si film on the sample is almost split off and the circles' shape is not same as that irradiated by the lower energy. Comparing with the un-patterned region (shown in figure 3.7 (d)), it's obvious that the nuclei position control is much better than the metal reflection layer method. And the uniform grain size would be useful in the device uniformity.

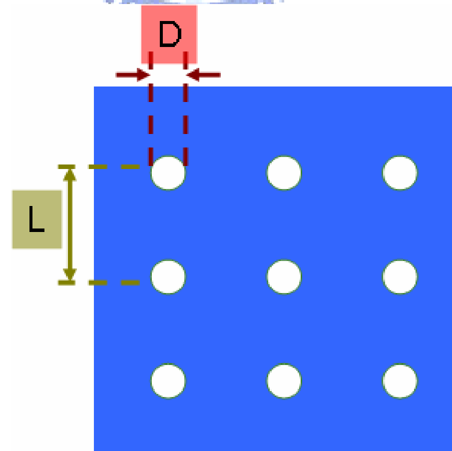

Figure 3.6 The top view of the nano-holes structure design. The value of D = 200nm and the value of L = 1μm.

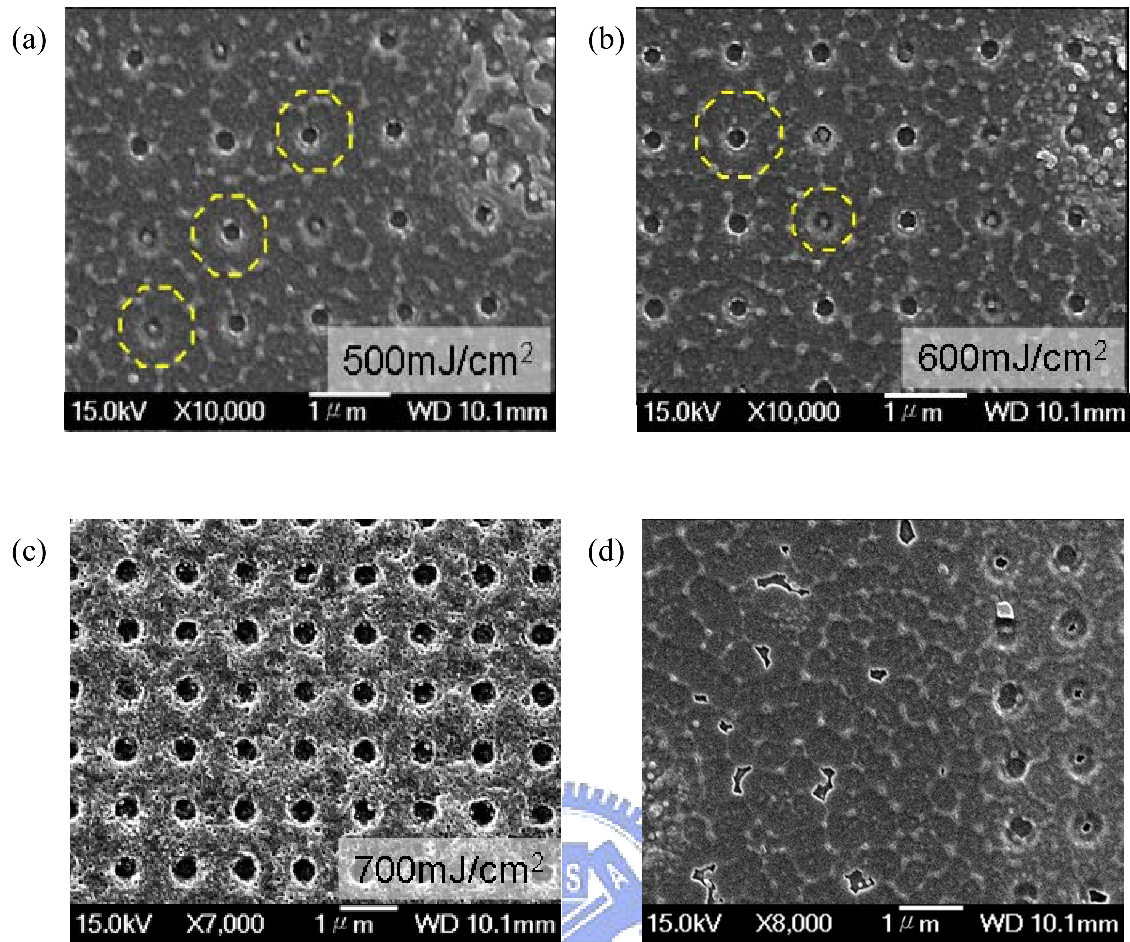

Figure 3.7 (a) The nano-hole region with L = 1μm and the laser energy = 500 mJ/cm^2. (b) The nano-hole region with L = 1μm and the laser energy = 600 mJ/cm^2. (c) The nano-hole region with L = 1μm and the laser energy = 700 mJ/cm^2. (d) The grain nuclei position control in the patterned region and unpatterned region.

3.3 Lateral grain growth induced by laser intensity distribution modulation with single slit diffraction

The single slit diffraction is a method which could induce a lateral grain growth by modulating the laser intensity distribution. It could modulate the laser input intensity distribution into the shape which could well induce the lateral grain growth. The original intensity distribution is a square-like shape and through the single-slit the intensity distribution would transfer to the form as

$$I = I_0 \cdot (\frac{\sin^2(\beta)}{(\beta)^2}) \quad , \qquad \text{where } \beta = \frac{\pi a \sin\theta}{\lambda} \quad \text{(shown in figure 3.8)}$$

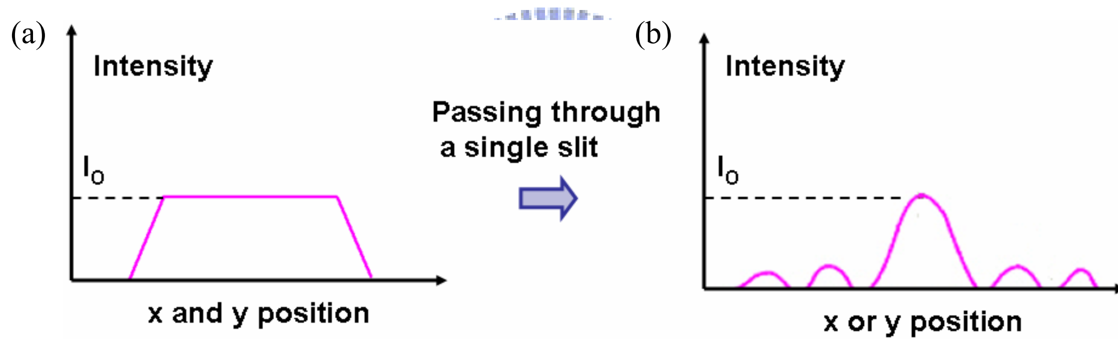

Figure 3.8 (a) the original laser intensity distribution (b) the laser intensity distribution.

Figure 3.9 is the full experimental procedure of the single slit diffraction. The buffer layer 7000Å SiO_2 and 1000Å α-Si was deposited on the cleaned Si wafer by furnace. The slit was fabricated by Al with thickness 0.1mm, and the slit width is 100μm, 150μm and 200μm shown in figure 3.10. We controlled the distance between the slit and the substrate by microslide. We changed the slit width and the distance between the substrate and the slit to modulate the final laser beam profile on the sample. We also changed the laser intensity at the same time such that we could well control the lateral grain growth position and the grain growth length.

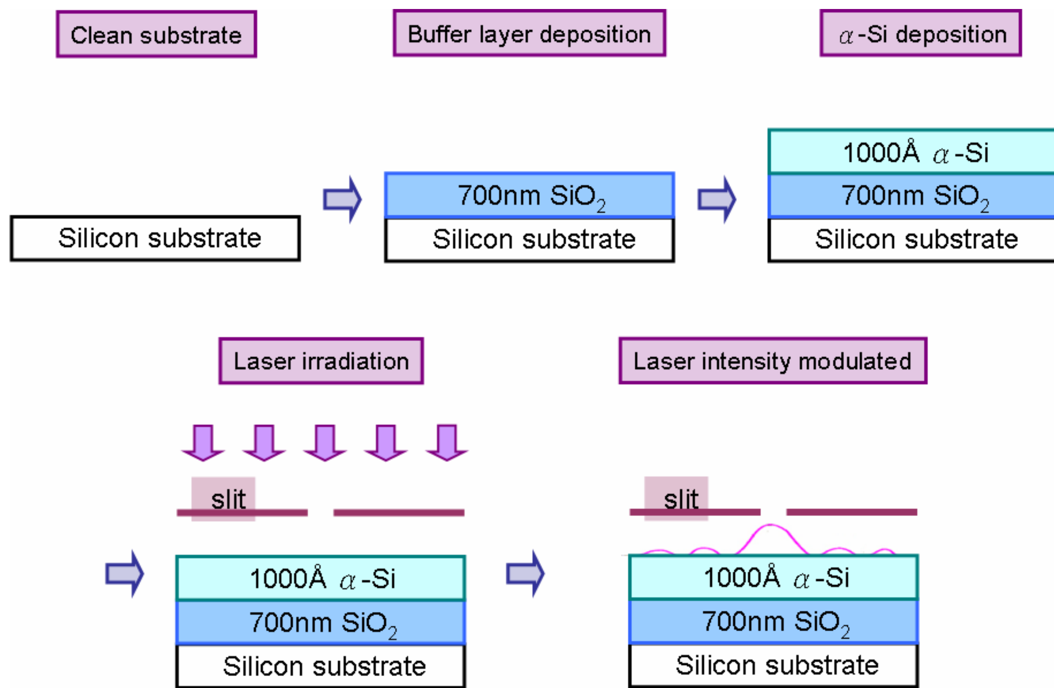

Figure 3.9 Full experiment procedure of lateral grain growth induced by single slit diffraction (including the sample preparation and laser irradiation).

Figure 3.10 (a) shows the region irradiated by the laser by the method of single slit diffraction. We could find that the laser intensity distribution was transferred to the form we expected. The laser energy of the region A is larger than that of the region B and in the higher laser intensity region C the Si has been split off. When the distance between the slit and the sample was too small, the phenomenon we mentioned before (figure 2.18) appeared (shown in figure 3.10 (b)). When the value of the slit width (represented by a) over the distance between the slit and the sample (represented by L) is larger than 55 the Fraunhofer diffraction could be observed. In the figure 3.10 (c) and (d), the lateral grain growth region could be distinguished easily. The "white lines" are the grain boundaries induced by the large grain growth.

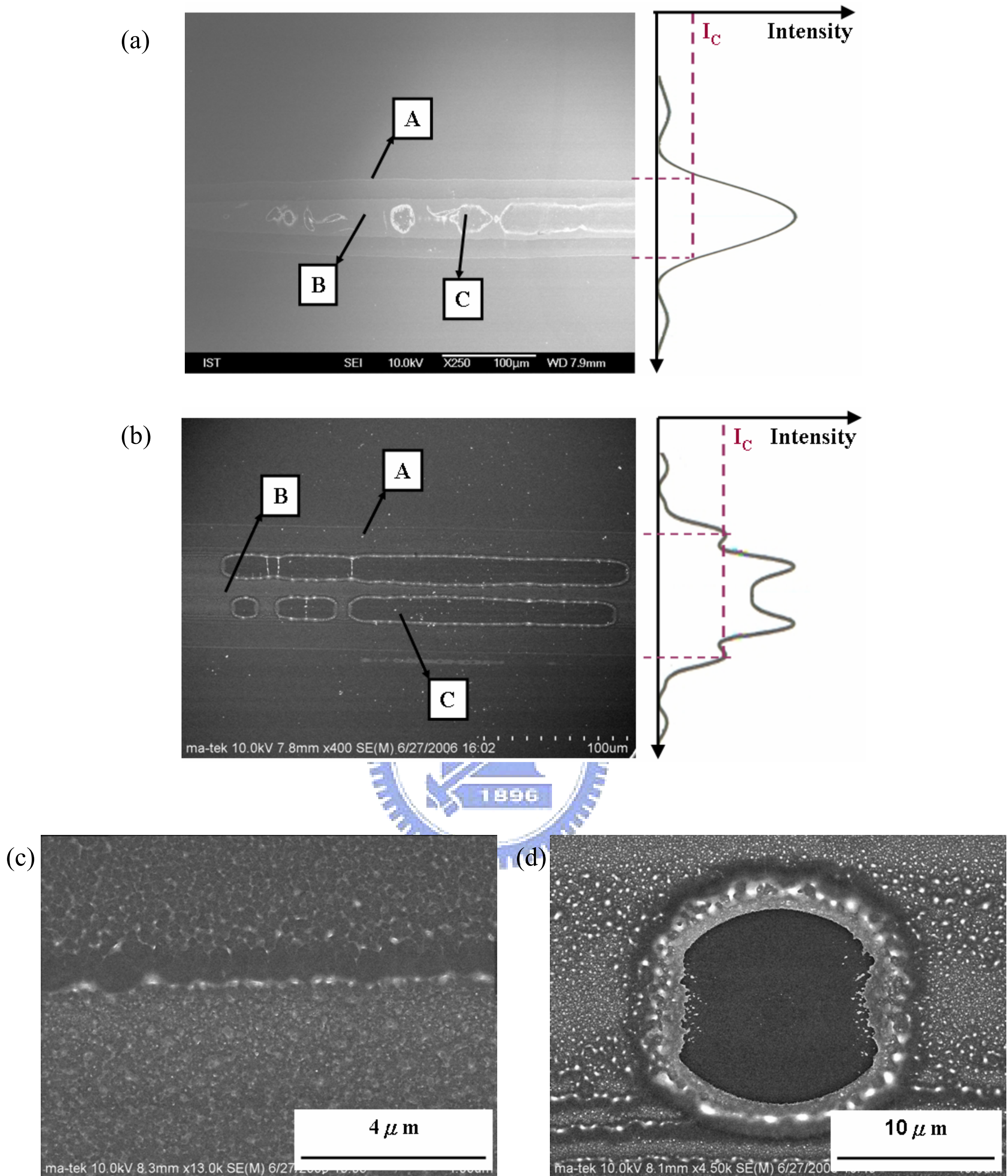

Figure 3.10 The broad view of region irradiated by the single slit diffraction method and the laser intensity distribution. I_C is the minimum intensity to crystallize the α-Si. (a) Fraunhofer (far field) diffraction. (b) Fresnel (near field) diffraction. (c) (d) The broad view of the lateral grain growth region and the white lines are the grain boundaries induced by the lateral grain growth.

(a)

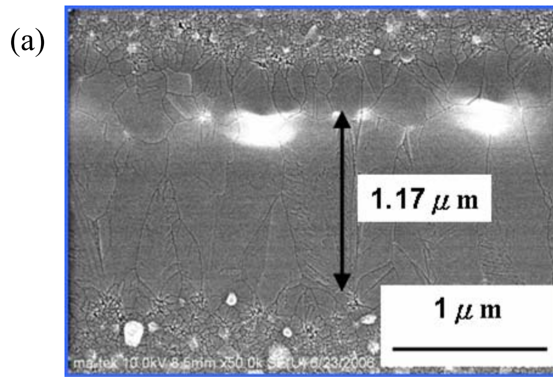

(c)

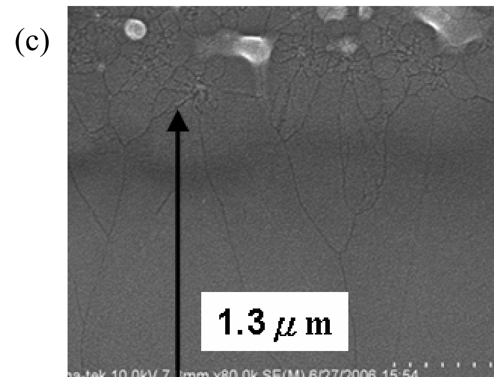

(b)

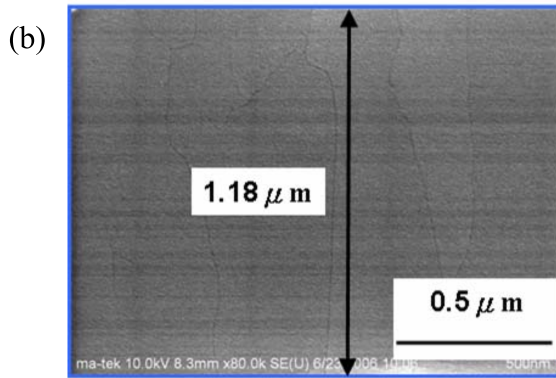

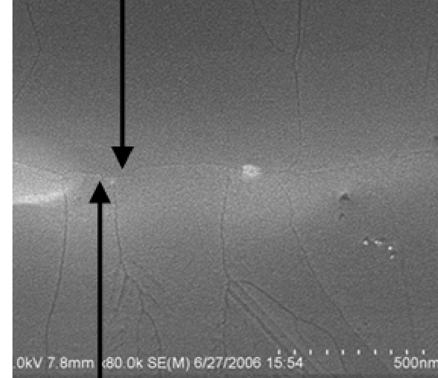

(d)

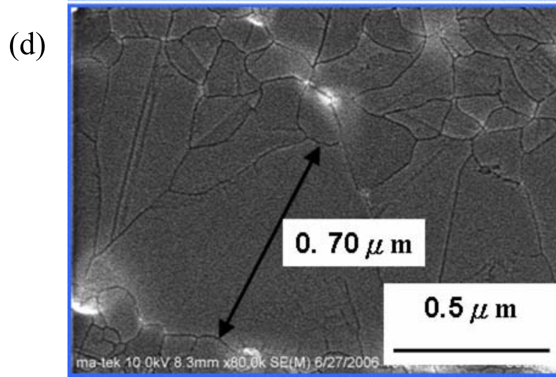

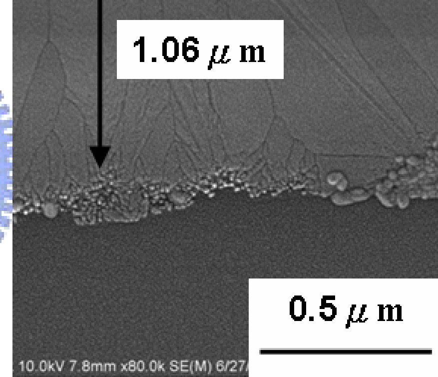

(e)

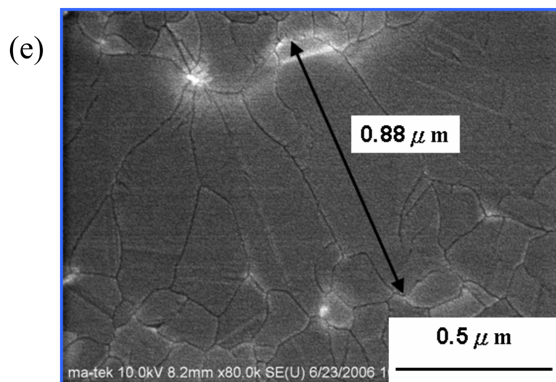

(f)

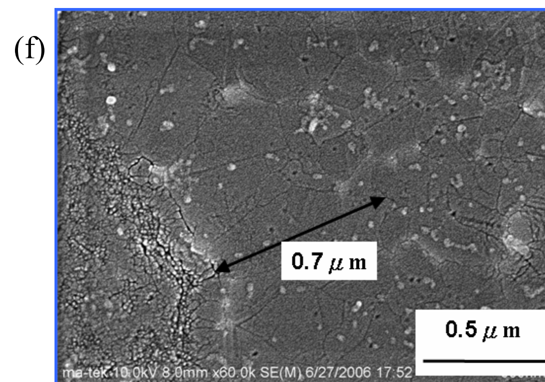

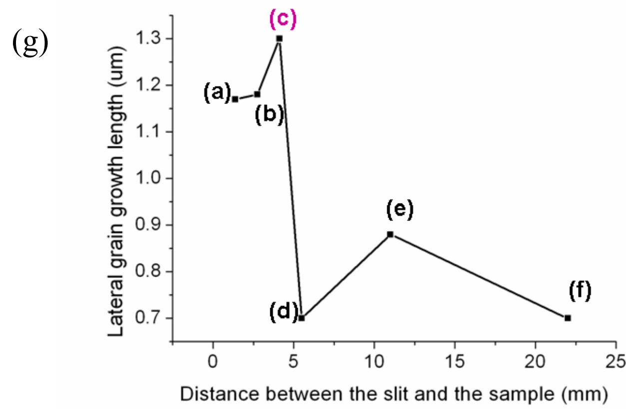

Figure 3.11 the SEM image for the different L: (a) L= 1.375mm (b) L = 2.75mm (c) L = 4.125mm (d) L = 5.5mm (e) L = 11mm (f) L = 22mm. (g) the lateral grain size versus L at the same laser energy 500mJ/cm^2.

The fine view of the lateral grain growth region is illustrated in figure 3.11. The laser intensity is not the critical parameter to influence the lateral grain growth length but it could decide the position of the lateral grain growth region. As long as the laser intensity is large enough the lateral grain growth length would depend on the laser intensity distribution induced by the diffraction critically. If the slope intensity is not large enough, the lateral grain growth would only occur in the region between the completely melting and partially melting region because the exceeding thermal energy in the completely melting region would transfer to the unmelting Si dramatically. If the slope of the intensity distribution could be modulated larger the longer lateral grain growth region would be obtained. Comparing figure 3.11 (c) and (f), the lateral grain growth length is 1.3μm and 0.7μm separately. The lateral grain size of (c) is almost two times that of (f) and (g) shows the optimum value of L at the same energy. In (f), the lateral crystallization phenomenon would not be so obvious because the intensity gradient is too small such that the lateral grain growth no longer occurs. We could only find that with the intensity increasing the grain size from the small grain region into the SLG and then transfer to the fine grain region (complete melting).